Journal of the Iranian Chemical Society
https://doi.org/10.1007/s13738-021-02298-6

ORIGINAL PAPER

Synthesis, density functional theory, and cytotoxic activity of some heterocyclic systems derived from 3-(3-(1,3-diphenyl-1*H*-pyrazol-4-yl) acryloyl)-2*H*-chromen-2-one

Sayed K. Ramadan[1] · **Sameh A. Rizk**[1]

Received: 16 January 2021 / Accepted: 29 May 2021

Abstract
The behavior and reactivity of a coumarin-based chalcone bearing a pyrazole core **3** toward malononitrile, hydrazine, thiourea, hydrazinecarbothioamide, 2-aminoaniline, and 6-aminothiouracil were investigated as an attempt to design and synthesize a novel series of pyrazole-based heterocycles, viz. pyranocoumarin, diazepine, pyrimidochromene, triazepine, benzodiazepine, and pyrimidopyrimidine derivatives. DFT based on quantum chemical computation outlines the structure optimization of the intermediate that reacted to achieve the desired product. The antitumor activity screening against HePG-2 and MCF-7 cancer cell lines disclosed that the most potent compounds against two cell lines were **9** and **17** as compared to doxorubicin which may be attributed to their presence in more tautomeric structures. Also, the minimized energy, dipole moment, ionization potential, transferred electrons, and charge density distribution disclosed that the greater value of 0.126 and 0.8 for pyrazole derivatives **9** and **17**, respectively, indicates the maximum transfer of electron and hence greater tendency of scavenging radicals and rapidly reduce oxygen to superoxide.

Keywords Chromene · Chromenodiazepine · Computational chemical study · Pyrimidopyrimidine · Triazepine

Introduction

Chalcones (1,3-diaryl-2-propane-1-ones) are secondary metabolites obtained from the main precursors of flavonoids and isoflavonoids biosynthesis occurred in terrestrial plants and associated with diverse biological effect [1]. Coumarins (naturally occurring oxygen heterocyclic compounds) and pyrazoles (nitrogen heterocyclic compounds) are of great importance due to their pharmacological effects like antioxidant, antiviral, antiproliferative, antimicrobial, and anti-inflammatory activities [2–16]. Recently, pyrimidines (an integral part of DNA and RNA) and their related fused heterocyclic systems exhibit antiviral, anti-influenza, antioxidant, anti-inflammatory, antimalarial, and antitumor properties [6–8, 17–21]. It is well known that chalcones are highly reactive due to α,β-unsaturated carbonyl functionality, which was a good synthon for the synthesis of five-, six-, and seven-membered ring systems [22]. Indeed, as an extension of our study of the reaction products and synthesis of some important biological heterocycles [23–41], this work aimed to investigate the behavior and reactivity of the chalcone bearing a coumarin moiety **3** toward some carbon and nitrogen nucleophiles under different aspects. It was found that chalcone **3** suffers from four electron-deficient centers attacked by the nucleophiles depending on the nature of the nucleophile and the reaction conditions (Fig. 1).

Results and discussion

Chemistry

Claisen–Schmidt condensation of 3-acetylcoumarin **1** with pyrazole aldehyde **2** [42] achieved the chalcone derivative **3** as yellow crystals (Scheme 1). The IR spectrum displayed coumarinyl C = O at ν 1722 cm^{-1} and ketonic C = O at ν 1655 cm^{-1}. Its ^{1}H NMR spectrum disclosed C5-H of pyrazole at δ 9.29 ppm, C4-H of coumarin at δ 8.65 ppm as well as the aromatic and olefinic protons. Further support for the assigned structure **3** was acquired from its mass spectrum

✉ Sayed K. Ramadan
sayed.karam2008@sci.asu.edu.eg

[1] Department of Chemistry, Faculty of Science, Ain Shams University, Cairo 11566, Egypt

Published online: 04 June 2021

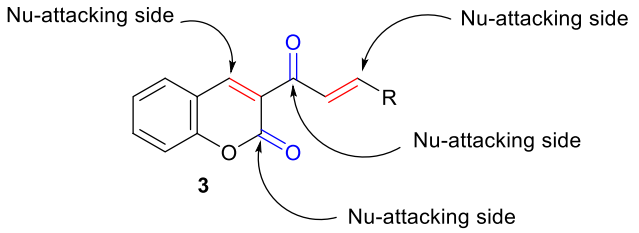

Fig. 1 Nucleophilic-attacking sides in coumarin-based chalcone **3**

which showed the correct molecular ion peak at *m/z* 418 (22%) and the base peak at *m/z* 77 (100%) corresponding to phenyl cation, in addition to some important fragments (cf. Experimental). Our research team was intrigued by studying the regioselectivity of the reaction products under different conditions [27–41]. Therefore, treating chalcone **3** with malononitrile in boiling ethanol and piperidine failed to produce 2-amino-3-cyanopyran derivative **4** and achieved the arylidene malononitrile **5** as a sole product which was identical in all respects with an authentic sample prepared from condensation of pyrazole aldehyde **2** with malononitrile at room temperature [43] (Scheme 1). The reaction pathway can be visualized via two routes as displayed in Scheme 2 (according to the plausible reaction mechanistic pathway) and Fig. 2 (according to the stability of both intermediates and final products). Noteworthy, the pyranochromene derivative **6** was obtained upon cyclocondensation of **5** with 4-hydroxycoumarin in boiling ethanol and triethylamine. The ^{1}H NMR spectrum of **6** revealed an exchangeable singlet signal for NH_2 and singlet for methine proton in addition to the aromatic protons (cf. Experimental). In turn, cyclocondensation reaction of **5** with thiourea in boiling ethanol including anhydrous potassium carbonate furnished 6-aminopyrimidin-5-carbonitrile derivative **7**. Its IR spectrum disclosed bands characteristic for NH, NH_2, C≡N, and C = N groups.

Otherwise, when chalcone **3** was treated with hydrazine in refluxing dioxane, chromenodiazepine derivative **9** was obtained instead of 3-coumarinyl-5-pyrazolylpyrazole derivative **8**. IR spectrum of **9** revealed the carbonyl functionalities at ν 1722 and 1676 cm^{-1}. In contrast, hydrazinolysis of chalcone **3** in boiling glacial acetic acid achieved the diazepinedione derivative **10** (Scheme 3). The chemical

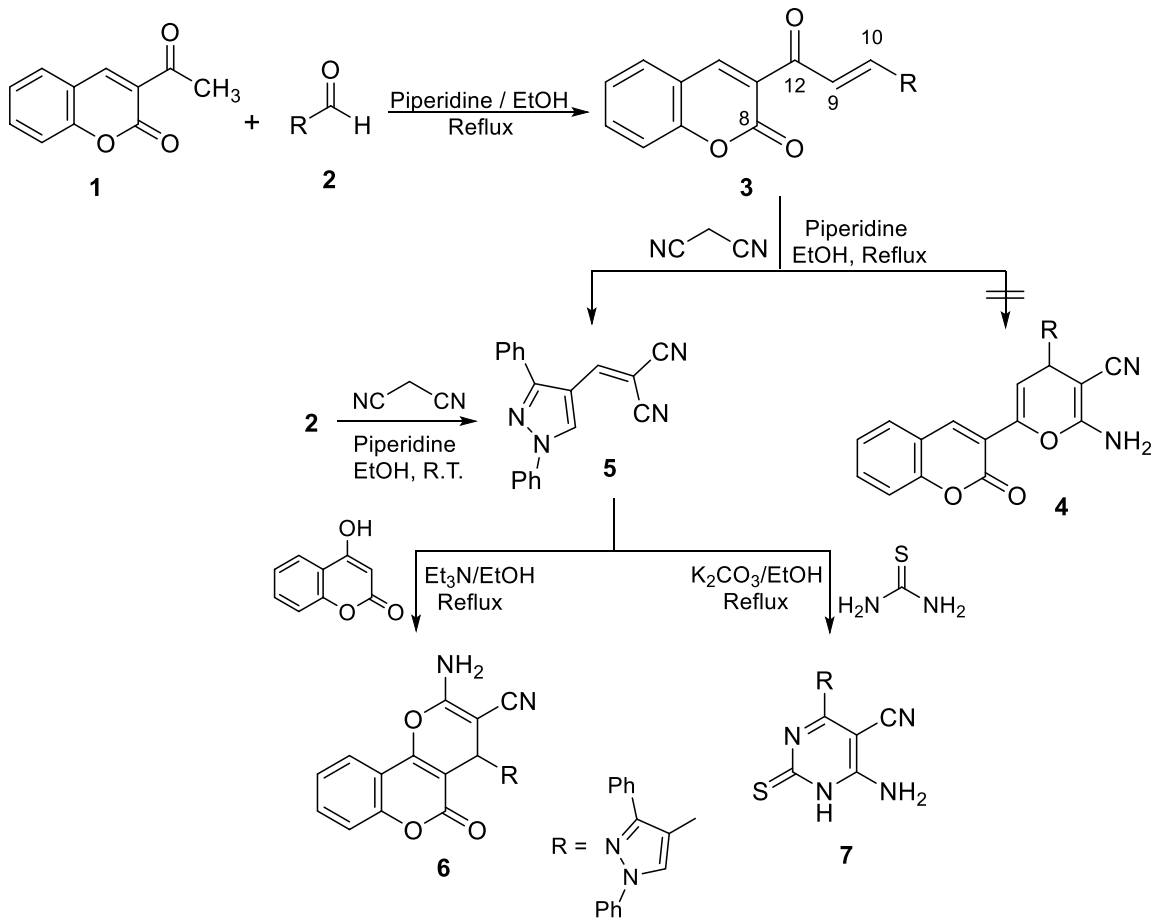

Scheme 1. Synthesis of chalcone **3** and compounds **5–7**

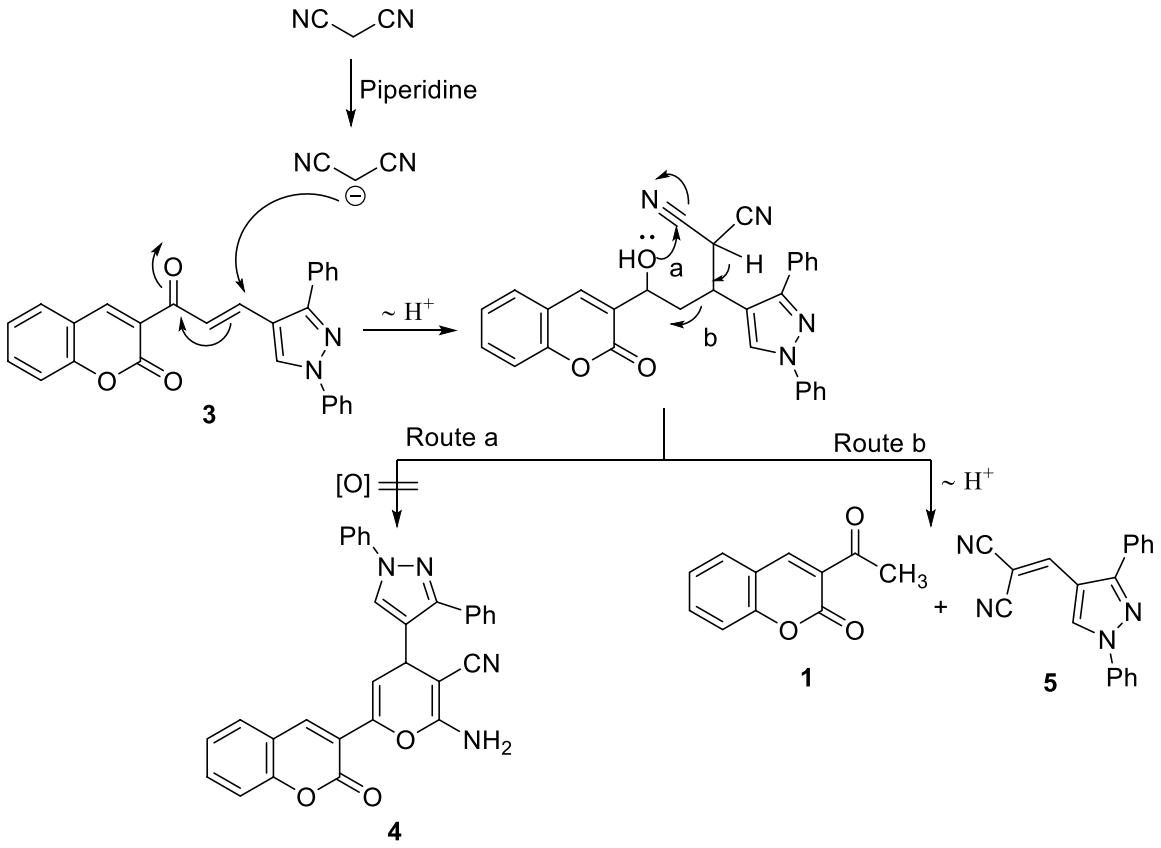

Scheme 2. Plausible pathways for the reaction of chalcone **3** with malononitrile

structures were substantiated from their analytical and spectral properties (cf. Experimental). The plausible pathways of hydrazinolysis reaction can proceed via two routes as depicted in Scheme 4.

The behavior of hydrazinolysis of chalcone **3** using different solvents to achieve compounds **9** and **10** instead of the pyrazole derivative **8** may be attributed to the electrophilicity of the C20 followed by C10 and C8 that are more electrophilic center than C12, respectively (cf. Fig. 3).

The reaction of chalcone **3** with thiourea was not successful in boiling dioxane while in boiling sodium ethoxide acquired the chromenopyrimidine derivative **12** instead of pyrimidinethione derivative **11** (Scheme 5). The IR spectrum was devoid of C = O of coumarin moiety and displayed ν C = O of amide at 1689 cm^{-1}. The reaction pathway can be extrapolated via Scheme 6.

Interaction of chalcone **3** with thiosemicarbazide in boiling dioxane failed to furnish the pyrazole derivative **13** and afforded the triazepinethione derivative **14** (Scheme 7). Its IR and ^{1}H NMR spectra were devoid of NH_2 bands. Further, the highest recorded peak in its mass spectrum was at *m/z* 489 (5%) corresponding to the correct molecular ion peak and the base peak at *m/z* 77 (100%) which is attributable to phenyl cation. In a similar manner, 2-aminoaniline reacted with chalcone **3** in boiling dioxane to provide benzodiazepine derivative **15**. In contrast, pyridopyrimidine derivative **17** was obtained instead of pyridopyrimidine derivative **16** upon treating chalcone **3** with 6-aminothiouracil in boiling dioxane including piperidine (Scheme 7). The IR spectra conserved the coumarin carbonyl functionality. The reactions can proceed via aza-Michael addition followed by ring closure by loss of water.

Density functional theory study

It is well known that high E_{HOMO} are likely to indicate a strong tendency of the molecule to donate electrons. The low values of the energy gap ($\Delta E = E_{LUMO} - E_{HOMO}$) will render good inhibition efficiencies because the energy needed to remove an electron from the last occupied orbital will be low [44]. Density functional theory (DFT) based on quantum chemical computation using Quantum espresso version 6.7 outlines the structure optimization of the intermediate that reacted to afford the desired product. In the presence of reaction of the coumarin chalcone with carbon nucleophile, e.g., malononitrile, the HOMO energy (−14.54 eV) rather than HOMO of nitrogen nucleophiles, e.g., hydrazine hydrate (−10.83 eV), thiourea (−8.96 eV)

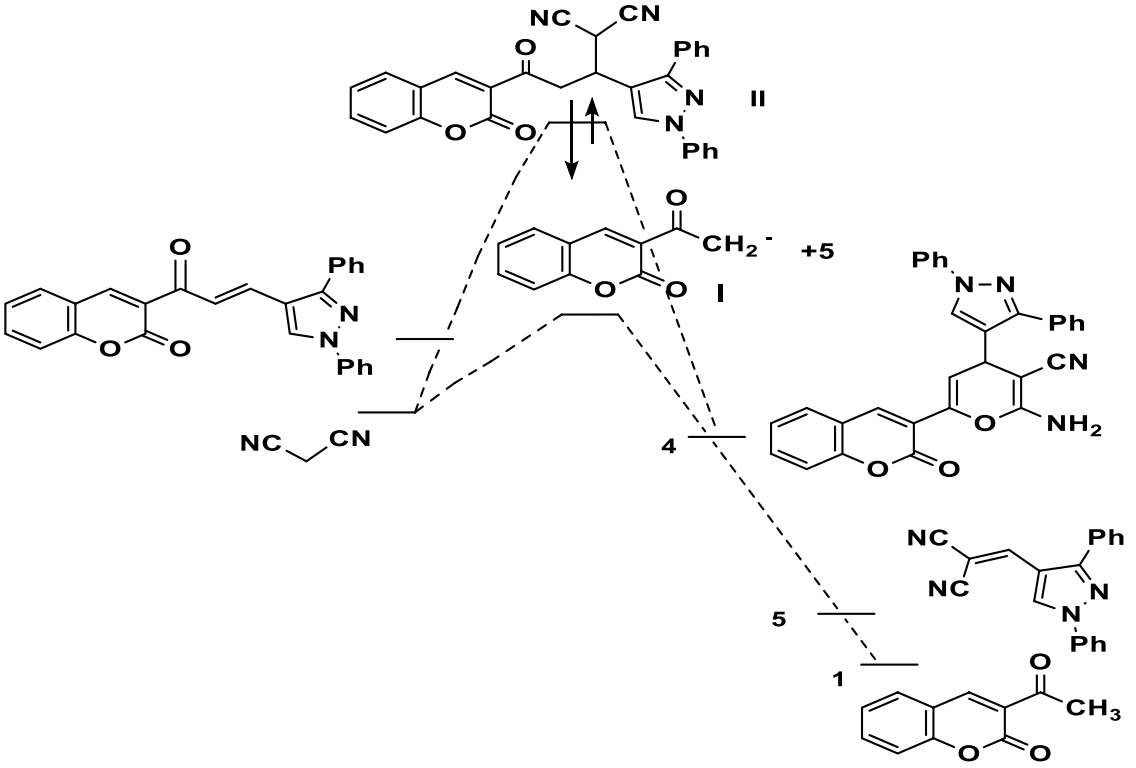

Fig. 2 Stability of the intermediates and final products

Scheme 3. Reactions of chalcone **3** with hydrazine under different conditions

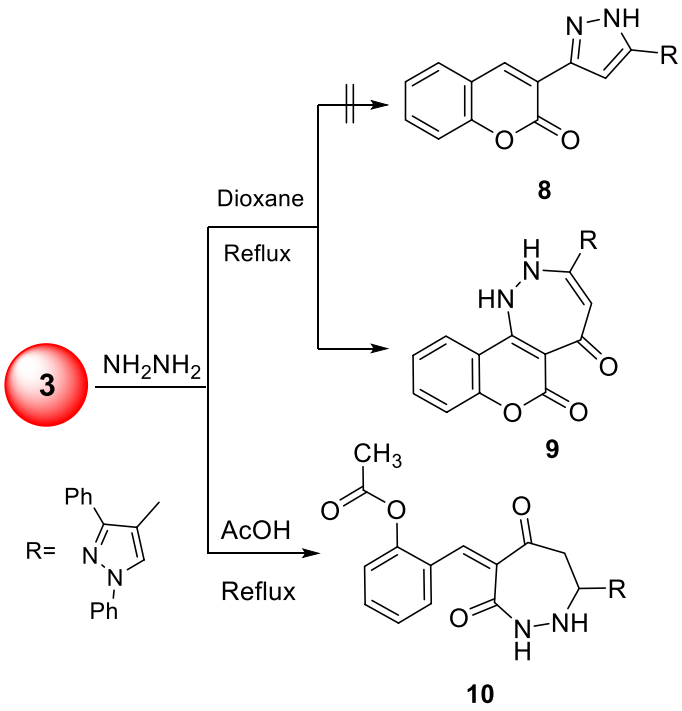

and 6-aminothiouracil (−9.05 eV) and so good matching to LUMO energy (−6.37 eV) of the carbonyl electrophilic site of chalcone to form the corresponding new heterocyclic via addition reaction followed by cyclization. In the case of using thiosemicarbazide (HOMO −5.32 eV) is more preferred than HOMO of *o*-phenylenediamine (−7.72 eV)

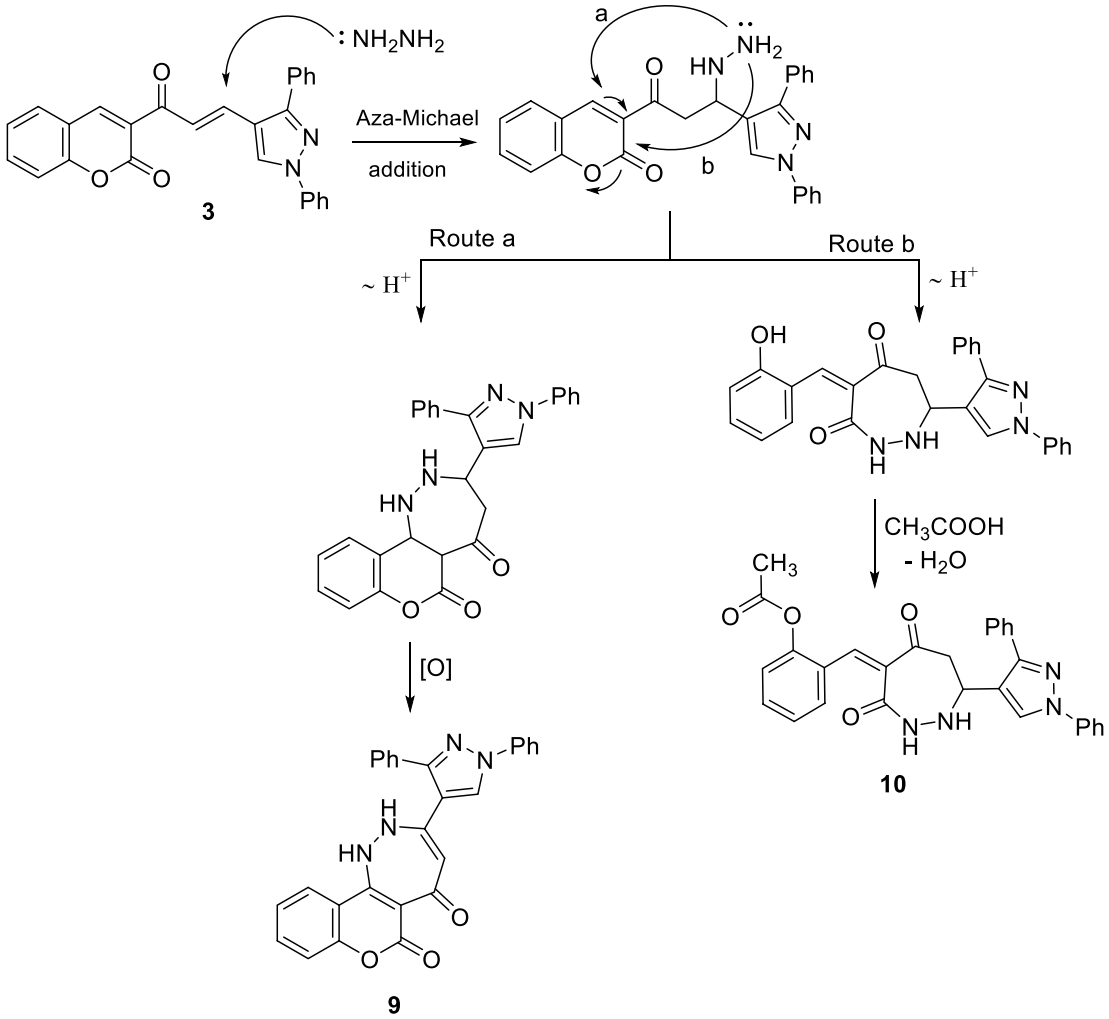

Scheme 4. Plausible pathways for formation of compounds **9** and **10**

proceeding via mechanism of Scheme 7 to form thermodynamically intermediate. This means in the case of malononitrile, it is a thermodynamic stable intermediate (cf. Figure 4).

So, DFT simulation helped us to know why the reactions of chalcone **3** with malononitrile, hydrazine hydrate, thiourea, thiosemicarbazide, and 6-aminothiouracil did not afford the expected heterocyclic compounds **4, 8, 11, 13,** and **16** and they yielded newly heterocyclic compounds **5, 9, 12, 14** and **17**, respectively. The structures have been supported by full spectral analysis and microanalytical data. Quantum chemical parameters calculation is using the density functional theory (DFT) method for the calculations of the newly synthesized compounds (Table 1). The high E_{HOMO} are likely to indicate a strong tendency of the molecule to donate electrons. The low values of the energy gap ($\Delta E = E_{LUMO} - E_{HOMO}$) will render good efficiencies [45]. The dipole moment, hardness, softness, and surface area (nm^2) for newly pyrazole derivatives carrying hydrophobic groups were agreed with an excellent explanation for the synthesized compounds and their anticancer efficiency. Also, the Ionization potential (I, eV), transferred electrons, and charge density distribution (ΔN) indicate the greater value pyrazole derivatives **5, 9, 12, 14,** and **17** have the maximum transfer of electron and hence, greater tendency of adsorption and inhibition for the cancer cell. The optimization structures of the synthesized pyrazole **3–17** are outlined in Fig. 5 (supplementary material). The coordinates of the optimized structures are given in Table 2 (cf. the supporting information).

The calculated ΔE was compared with the theoretical reference data based on the corresponding experimental results in gas phase reaction. With ΔE being a criterion, three most typical and popular exchange–correlation functionals, e.g., PW91 were systematically compared in terms of the typical pyrazole, and diazepine synthesis in gas phase via reactions of chalcone of coumarin with hydrazine hydrate, thiourea, thiosemicarbazide and 2-aminouracil in the presence of different solvents, e.g., dioxane, acetic acid and ethanol

Atom	Charge (Huckel)
C(1)	-0.013098
C(2)	0.270053
C(3)	-0.0995856
C(4)	-0.012039
C(5)	-0.0736049
C(6)	-0.0217486
O(7)	-0.0260278
C(8)	0.539133
C(9)	-0.0601339
C(10)	0.0806652
O(11)	-0.572867
C(12)	0.368307
C(13)	-0.234696
O(14)	-0.720942
C(15)	0.128725
N(16)	-0.353525
N(17)	0.780241
C(18)	-0.109348
C(19)	-0.0835804
C(20)	0.0335314
C(21)	0.154601
C(22)	-0.0912975
C(23)	-0.0262466
C(24)	-0.083207
C(25)	-0.0268931

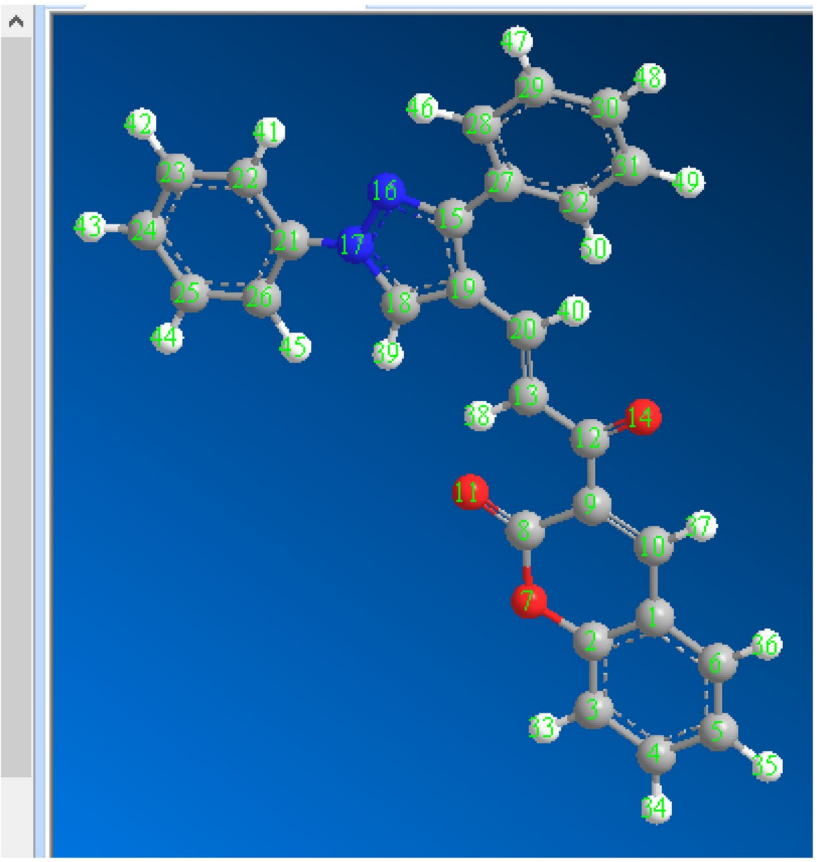

Fig. 3 Electrophilicity of carbon atoms in chalcone **3**

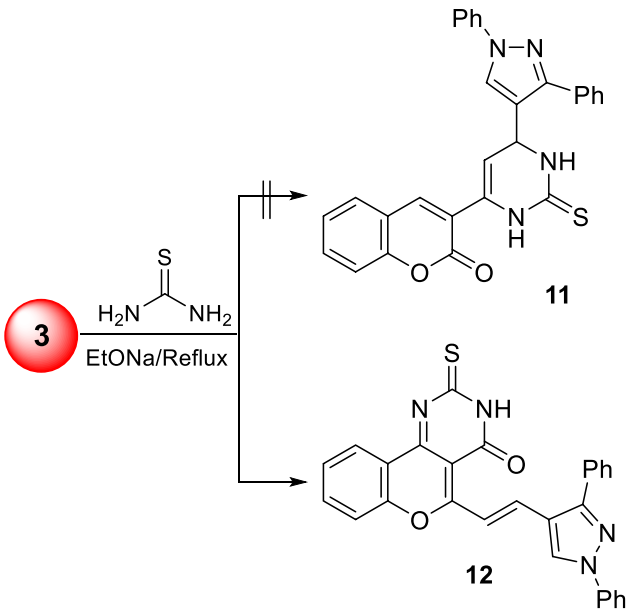

Scheme 5. Reactions of Chalcone **3** with thiourea

motorized via piperidine and sodium ethoxide. In addition, the verifications of geometrical and electronic properties of modeling the anticancer products, as well as the adsorption behaviors of typical probe reactants and solvents are also suggested for further screening proper functionalization. The present work shows general implications for how to choose a reliable exchange–correlation functional in the computational solvents and catalyst on reactant surface.

Quantum chemical parameter calculations using density functional theory (DFT) method used for the calculations of the synthesized compounds are in good agreement with the anticancer efficiency (Table 1). The listed results indicated that the values of gap energy (ΔE), where $\Delta E = E_{\mathrm{LUMO}} - E_{\mathrm{HOMO}}$ follow the order: heterocyclic derivatives **9** < **17** < doxorubicin. Compounds having small ΔE values are generally referred to as soft compounds that are more reactive toward radical surface interactions, being capable of donating electrons easily to hole surface [46]. Not only the scavenging ability toward positive hole, tumor, radical, and oxygen removable depended upon E_{HOMO} values, but also the number of heteroatoms, electron distributions, surface area, and lipophilicity must be considered. The dipole moment, softness (σ, eV^{-1}), and surface area (nm^2)

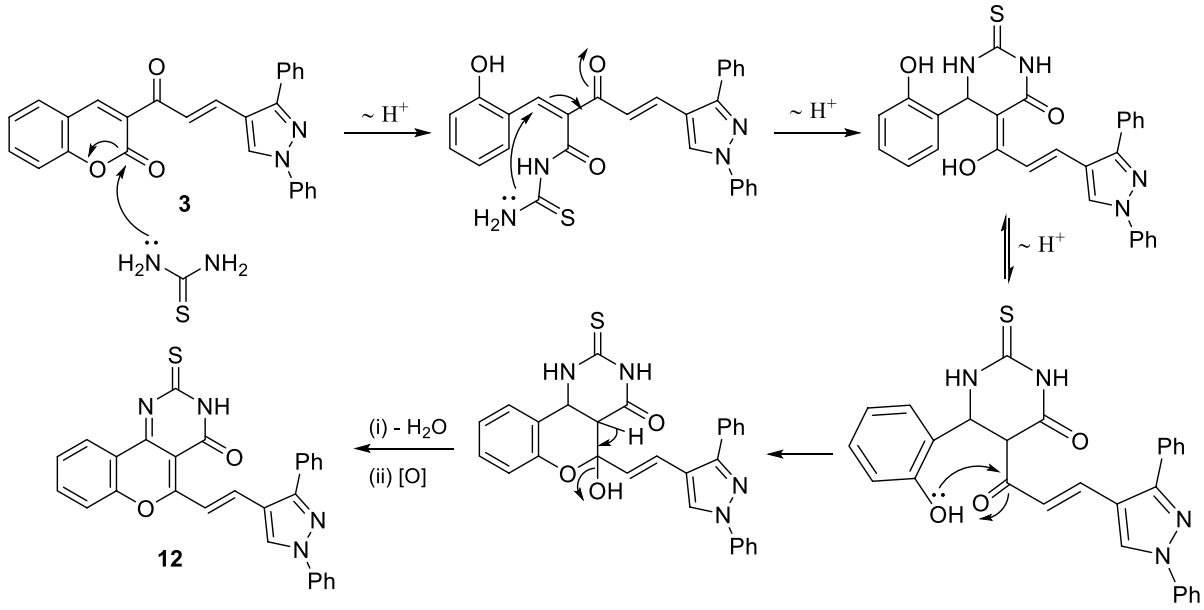

Scheme 6. A suggested pathway for compound **12**

for most potent synthesized compounds carrying hydrophobic groups were agreed to an excellent correlation between oxidation inhibition efficiencies.

On the other hand, the minimized energy (kcal/mol), dipole moment, ionization potential (I, eV), transferred electrons, and charge density distribution (ΔN) revealed that the greater value of 0.126 and 0.8 for pyrazole **9** and **17**, respectively, indicates the maximum transfer of electron and, hence, greater tendency of scavenging radicals and rapidly reduces oxygen to superoxide (O2•–) [47] (see more in Table 1). The comparison between the Mulliken total atomic charges of first 20 atoms for compounds **(11, 12, 13, 14, 16** and **17)** is depicted in Fig. 4.

Biological screening

It was shown that several enzymes including the cytochrome P450 reductase, NADH dehydrogenase, and xanthine oxidoreductase could reduce doxorubicin via a one-electron reduction mechanism giving rise to the phenate radical intermediate that can rapidly reduce oxygen to superoxide ($O_2^{\bullet-}$) via a futile redox-cycling mechanism [48]. In the presence of a redox-active metal ion such as iron (III), hydroxyl radicals are formed via the Fenton mechanism. Chelators like desferrioxamine inhibit the formation of hydroxyl radicals through inhibition of the Haber–Weiss mechanism (Fig. 5). Based on these in vitro studies, redox activation of newly synthesized compounds **9** and **17** to $O_2^{\bullet-}$, hydrogen peroxide (H_2O_2), and iron-catalyzed hydroxyl radical formation was suggested to be a similar mechanism of doxorubicin toxicity [47]. Oxidative stress is thought to be primarily responsible for phenolic diazepine **9**, pyrimidinethiol **17,** and doxorubicin cardiotoxicity because the myocardial tissues lack sufficient antioxidant mechanisms [49]. Compounds **9** and **17** are the stronger anticancer than the other synthesized compounds which may be due to their presence in more tautomeric structures (Table 2, Fig. 6).

Pharmacology

Antiproliferative screening

The antitumor activity screening of the synthesized compounds was measured against two cell lines, namely hepatocellular carcinoma (HePG-2) and mammary gland breast cancer (MCF-7), using MTT assay [50, 51]. The results in Table 3 and Fig. 7 disclosed that the most potent compounds against two cell lines were **9** and **17** as compared to doxorubicin. The compounds **6, 12,** and **15** were moderately potent against HePG-2 cell line. Moderate activity was displayed against MCF-7 cell line by the compounds **12, 14,** and **15**. The rest of compounds were of weak activity.

Conclusion

The behavior and reactivity of coumarin-based chalcone bearing a pyrazole core were investigated toward some carbon and nitrogen nucleophiles under different reaction conditions to synthesize a new series of fused and pyrazole-based heterocyclic systems like chromenopyran, chromenodiazepine, diazepine, chromenopyrimidine, triazepinethione, benzodiazepine,

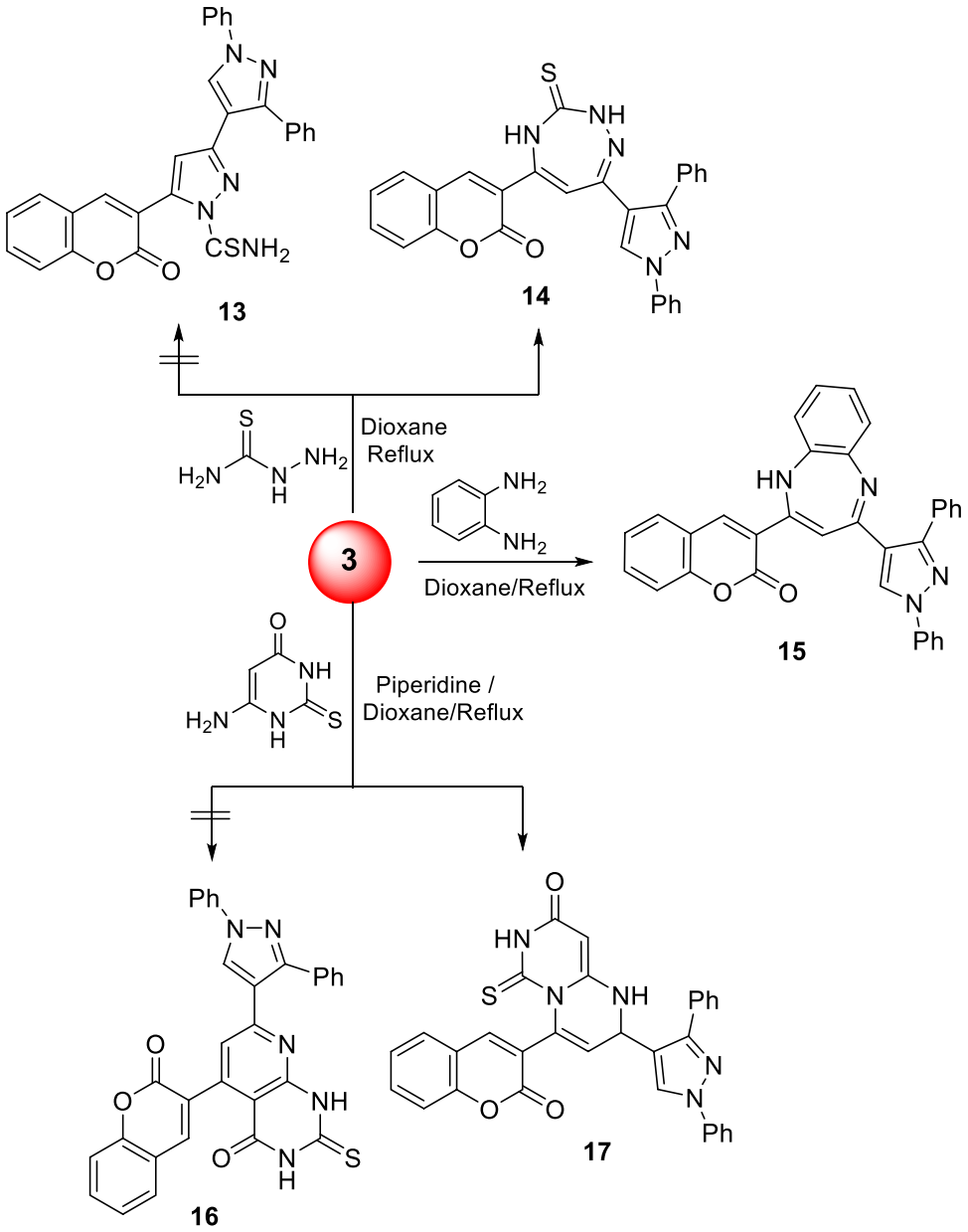

Scheme 7. Reactions of chalcone **3** with thiosemicarbazide, 2-aminoaniline, and 6-aminothiouracil

and pyrimidopyrimidine derivatives. The antitumor activity screening disclosed that the chromenodiazepine and pyrimidopyrimidine derivatives were the most potent against the two tumor cells, HepG-2 and MCF-7. DFT based on quantum chemical computation outlines the structure optimization of the intermediate that reacted to afford the desired product.

Experimental

General

All melting points were measured on a GALLENKAMP electric melting point apparatus and are uncorrected. Chemicals and solvents used were obtained from commercial sources and used as received or dried by standard procedures. IR spectra (ν, cm^{-1}) were recorded using potassium bromide disks on Fourier Transform Infrared Thermo Electron Nicolet iS10 Spectrometer (Thermo Fisher Scientific Inc., Waltham, MA, USA) at Faculty of Science, Ain Shams University. The ^1H NMR spectra (δ_H, ppm) were recorded at 300 MHz on a Varian GEMINI (GEMINI, Manufacturing & Engineering Inc., Anaheim, CA, USA) utilizing tetramethyl silane (TMS) as an internal standard in deuterated dimethyl sulfoxide (DMSO-d_6) at Faculty of Science, Cairo University. The mass spectra (MS) were recorded on Shimadzu GC-MS-QP-1000 EX mass spectrometer (Shimadzu Scientific Instruments,

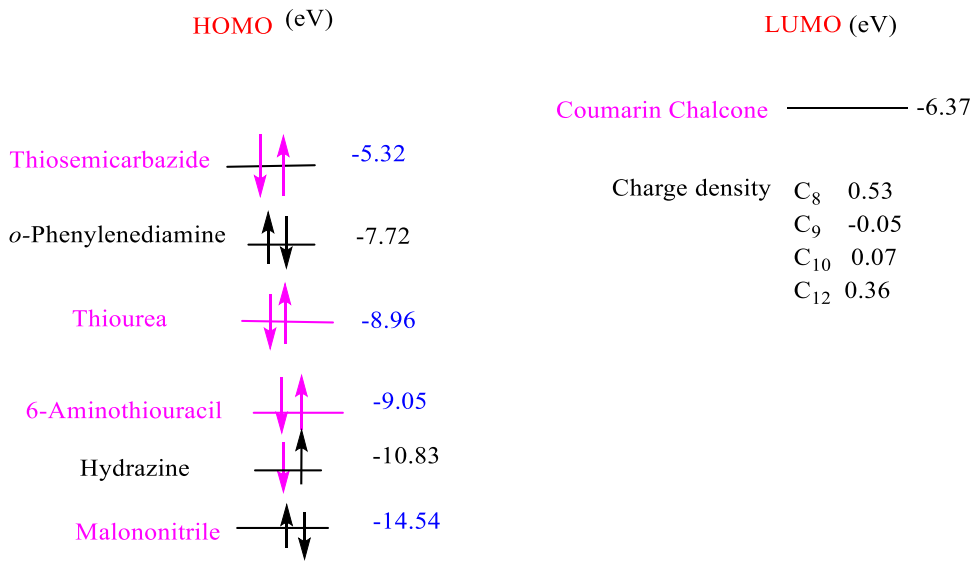

Fig. 4 Outline of the E_{HOMO} of nucleophiles toward E_{LUMO} of the starting material

Table 1 Global reactivity indices and energy level distribution of frontier orbitals

Compound	E_{HOMO}	E_{LUMO}	ΔE	I^a	A^b	μ^c	η^d	ω^e	ΔN^f	S^g	A_{molec} (nm^2)
3	−7.66	−6.14	1.52	7.09	5.38	7.29	0.76	35.60	0.028	1.34	232.246
4	−7.95	−5.70	2.25	8.08	5.93	16.39	1.13	21.56	0.046	0.88	364.594
5	−7.67	−4.40	3.27	7.36	4.36	6.62	1.63	13.366	0.0748	0.61	863.013
6	−7.80	−3.53	4.27	8.03	3.29	7.77	2.14	13.88	0.0720	0.46	761.829
7	−8.88	−2.67	6.21	8.69	2.78	6.13	3.16	102.6	0.023	0.39	232.246
8	−9.38	−4.53	4.85	9.65	4.85	7.03	2.51	62.02	0.017	0.398	265.246
9	−4.754	−3.604	1.15	4.96	3.82	4.23	0.60	5.36	0.126	1.67	609.594
10	−8.41	−2.96	5.45	7.36	4.36	5.86	2.83	48.59	0.095	0.349	493.013
11	−7.75	−4.98	2.77	7.66	4.66	4.04	1.39	12.94	0.077	0.719	687.625
12	−7.67	−4.56	3.11	7.63	4.24	−3.51	1.55	11.65	0.086	0.645	756.888
13	−7.46	−4.35	3.11	7.49	4.38	3.25	1.56	11.49	0.087	0.64	488.744
14	−5.40	−5.15	0.25	5.88	5.23	8.24	0.13	113.78	0.0087	7.69	377.146
15	−7.25	−4.67	2.58	7.26	4.66	5.14	1.29	10.24	0.09776	0.775	491.093
16	−6.88	−4.69	2.19	6.73	4.39	2.67	1.10	13.62	0.073	0.909	344.641
17	−7.51	−4.62	2.89	7.62	4.38	0.43	1.45	12.42	0.80	0.689	411.210

[a]Ionization potential
[b]Electron affinity
[c]Chemical potential
[d]Hardness
[e]Electrophilicity index
[f] nucleophilicity index
[g]Softness

Inc., USA) operating at 70 eV at the Regional Center for Mycology and Biotechnology (RCMB) of Al-Azhar University, Cairo, Egypt. The reactions were monitored by thin-layer chromatography (TLC) using Merck Kiesel gel 60 F_{254} analytical sheets obtained from Fluka, Switzerland. The starting pyrazole-4-carbaldehyde derivative **2** was previously prepared [42].

3-(3-(1,3-Diphenyl-1H-pyrazol-4-yl) acryloyl)-2H-chromen-2-one (3)

A mixture of 3-acetylcoumarin **1** (0.05 mol) and pyrazole aldehyde **2** (0.05 mol) in absolute ethanol (20 mL) including piperidine (0.1 mL) was refluxed for 2 h. The solid obtained while hot was filtered off and recrystallized from *n*-butanol

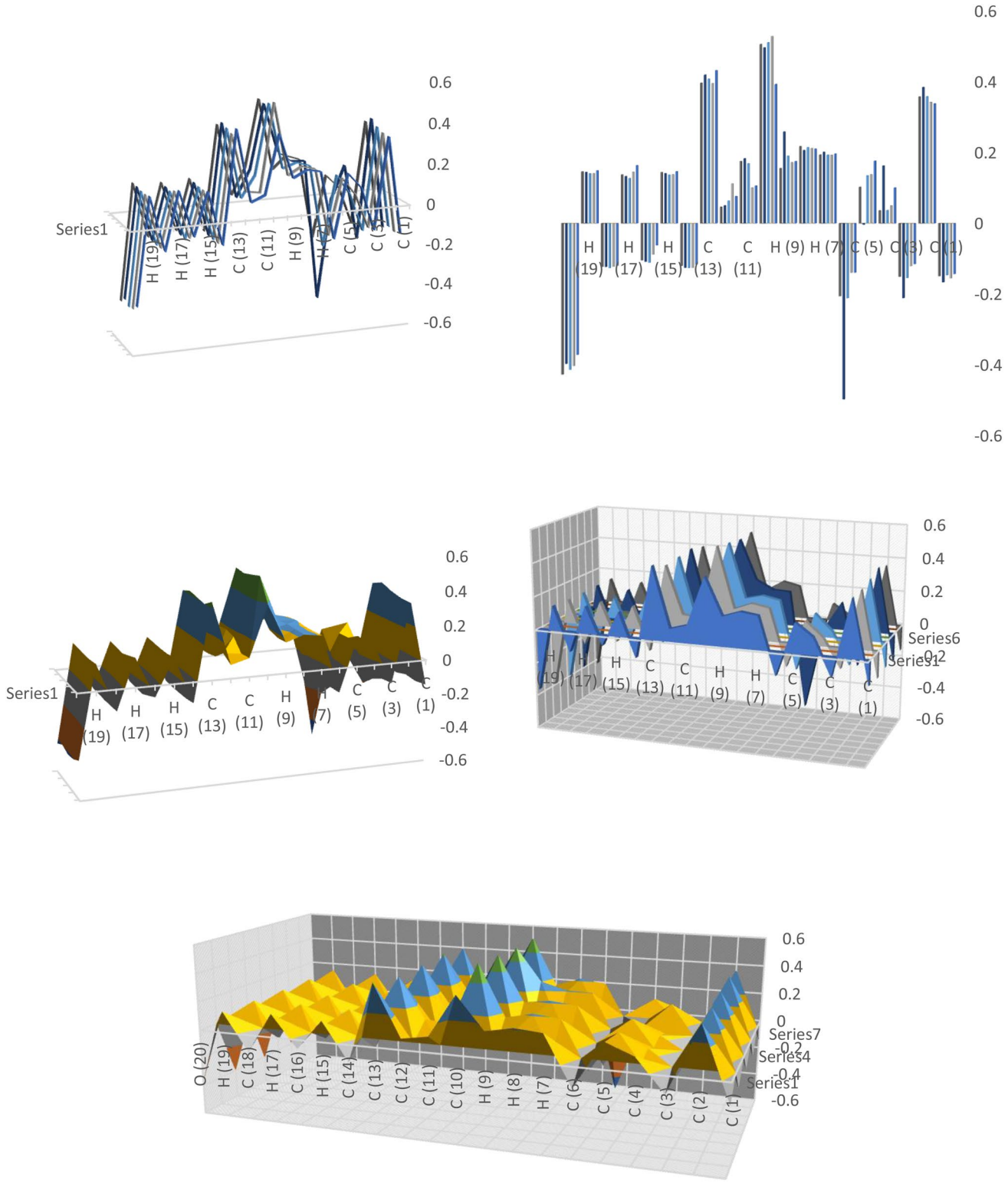

Fig. 5 Comparison between the Mulliken total atomic charges of first 20 atoms for compounds (**11, 12, 13, 14, 16** and **17**)

to furnish chalcone **3** as yellow crystals, mp. 260–262 °C, yield 90%. IR: 3059 (Arom-H), 1722 (C = O coumarin), 1655 (C = O ketone). ^{1}H NMR (300 MHz, DMSO-d_6): 9.29 (s, 1H, C5-H pyrazole), 8.65 (s, 1H, C4-H coumarin), 8.00–7.40 (m, 16H, Ar–H). MS, *m/z* (%): 418 ($M^{+\cdot}$, 22), 341 (4), 268 (9), 245 (89), 173 (25), 115 (26), 77 (100). Anal.

Table 2 Outline of the minimized energy and electron density of the tautomers of the more effective anticancer compounds **9** and **17**

Compound	$E_{Cal/mol}$	ΔE_{eV}	μ_{Dipole}	$e_{Charge\ density}$ diazepine N_{11}, N_{12}	E_{HOMO}	E_{LUMO}	$e_{Charge\ density}$ pyrimidine $N_{6\ bridge\ head}$
9a	78.70	1.21	15.55	0.246, 0.256	0.753	1.746	
9b	67.67	1.28	4.08	0.807, 0.434	−2.74	−4.02	
17a	69.5	2.89	0.43		−7.51	−4.62	0.468
17b	90.1	2.20	3.6		−7.0	−4.8	0.616
17c	102.0	6.6	6.6	−6.70 −4.50 0.587			

Calcd. for $C_{27}H_{18}N_2O_3$ (418.45): C, 77.50; H, 4.34; N, 6.69. found: C, 77.32; H, 4.27; N, 6.71%.

Reaction of chalcone 3 with malononitrile

A mixture of Chalcone **3** (0.01 mol) and malononitrile (0.01 mol) containing piperidine (0.1 mL) in dioxane (15 mL) was refluxed for 8 h. The solid was filtered off and crystallized from petroleum ether (80–100) and found to be *2-((1,3-diphenyl-1H-pyrazol-4-yl)methylene)malononitrile* ***(5)*** as yellow crystals, mp. 208–210 °C, (Lit. [43] mp. 210–212 °C), yield 88%.

2-Amino-4-(1,3-diphenyl-1H-pyrazol-4-yl)-5-oxo-4H, 5H-pyrano[3,2-c]chromene-3-carbonitrile (6)

A mixture of arylidine malononitrile **5** (0.01 mol) and 4-hydroxycoumarin (0.01 mol) in absolute ethanol (20 mL) including triethylamine (0.1 mL) was refluxed for 10 h (TLC), the contents were poured onto ice-cold water and then acidified by dil. HCl (10%). The deposited solid was filtered off and gray crystals were obtained after crystallization from ethanol, mp. 228–230 °C, yield 57%. IR: 3392, 3318 (NH_2), 2193 (C≡N), 1710 (C = O coumarin). ^{1}H NMR (300 MHz, DMSO-d_6): 8.58 (s, 1H, C5-H pyrazole), 7.87–7.29 (m, 14H, Ar–H), 7.26 (br.s, 2H, NH_2, exchangeable), 4.70 (s, 1H, C4-H pyran). MS, *m/z* (%): 458 ($M^{+\cdot}$, 22), 419 (8), 393 (59), 392 (100), 315 (19), 270 (30), 243 (21), 120 (14), 92 (41), 77 (55). Anal. Calcd. for $C_{28}H_{18}N_4O_3$ (458.48): C, 73.35; H, 3.96; N, 12.22. found: C, 73.22; H, 3.89; N, 12.25%.

6-Amino-4-(1,3-diphenyl-1H-pyrazol-4-yl)-2-thioxo-1,2-dihydropyrimidine-5-carbonitrile (7)

A solution of **5** (0.01 mol) and thiourea (0.01 mol) in absolute ethanol (20 mL) containing anhydrous potassium carbonate (0.01 mol) was heated under reflux for 6 h. The deposited solid was collected and recrystallized from ethanol to afford compound **7** as yellow crystals, mp. 170–172 °C, yield 68%. IR: 3375, 3250, 3175 (NH,NH_2), 2195 (C≡N), 1621 (C = N). ^{1}H NMR (300 MHz, DMSO-d_6): 8.73 (s, 1H, C5-H pyrazole), 7.98–7.22 (m, 10H, Ar–H), 7.10 (br.s, 2H, NH_2, exchangeable), 6.42 (br.s, 1H, NH, exchangeable). Anal. Calcd. for $C_{20}H_{14}N_6S$ (370.43): C, 64.85; H, 3.81; N, 22.69. found: C, 64.71; H, 3.75; N, 22.72%.

3-(1,3-Diphenyl-1H-pyrazol-4-yl)-1,2-dihydrochromeno[4,3-c][1,2]diazepine-5,6-dione (9)

A solution of Chalcone **3** (0.01 mol) and hydrazine hydrate (0.012 mol, 80%) in dioxane (15 mL) was refluxed for 8 h (TLC). The deposited solid was filtered off and off-white crystals were obtained after recrystallization from ethanol, mp. 240–242 °C, yield 52%. IR: 3142 (NH), 1722, 1676 (C = O). ^{1}H NMR (300 MHz, DMSO-d_6): 11.19 (br.s, 1H, NH, exchangeable), 9.23 (br.s, 1H, NH, exchangeable), 9.13 (s, 1H, C5-H pyrazole), 8.68 (s, 1H, = CH-CO), 8.00–7.39 (m, 14H, Ar–H). MS, *m/z* (%): 446 ($M^{+\cdot}$, 11), 433 (21), 387 (26), 355 (31), 312 (46), 246 (34), 138 (16), 88 (32), 77 (100). Anal. Calcd. for $C_{27}H_{18}N_4O_3$ (446.47): C, 72.64; H, 4.06; N, 12.55. found: C, 72.51; H, 3.97; N, 12.51%.

2-((7-(1,3-Diphenyl-1H-pyrazol-4-yl)-3,5-dioxo-1,2-diazepan-4-ylidene)methyl)phenyl acetate (10)

A solution of Chalcone **3** (0.01 mol) and hydrazine hydrate (0.012 mol, 80%) in glacial acetic acid (10 mL) was refluxed for 4 h (TLC). After cooling, the reaction mixture was poured onto ice-cold water. The solid obtained was filtered off and yellow crystals were obtained after crystallization from ethanol, mp. 296–298 °C, yield 69%. IR: 3127 (NH), 1734 (C = O ester), 1657 (C = O). ^{1}H NMR (300 MHz, DMSO-d_6): 8.54 (s, 1H, C5-H pyrazole), 8.34 (s, 1H, CH=), 7.89–7.27 (m, 16H, Ar–H + 2NH), 5.76–5.70 (dd, 1H, CHNH), 3.98–3.88 (dd, 1H, 1H of CH_2), 3.28–3.22 (dd, 1H, 1H of CH_2), 2.33 (s, 3H, CH_3). MS, *m/z* (%): 492 ($M^{+\cdot}$, 29), 491 (47), 474 (97), 431 (82), 353 (22), 241 (26), 220 (100), 155 (17), 104 (26), 77 (28). Anal. Calcd. for $C_{29}H_{24}N_4O_4$ (492.54): C, 70.72; H, 4.91; N, 11.38. found: C, 70.92; H, 4.49; N, 11.38%.

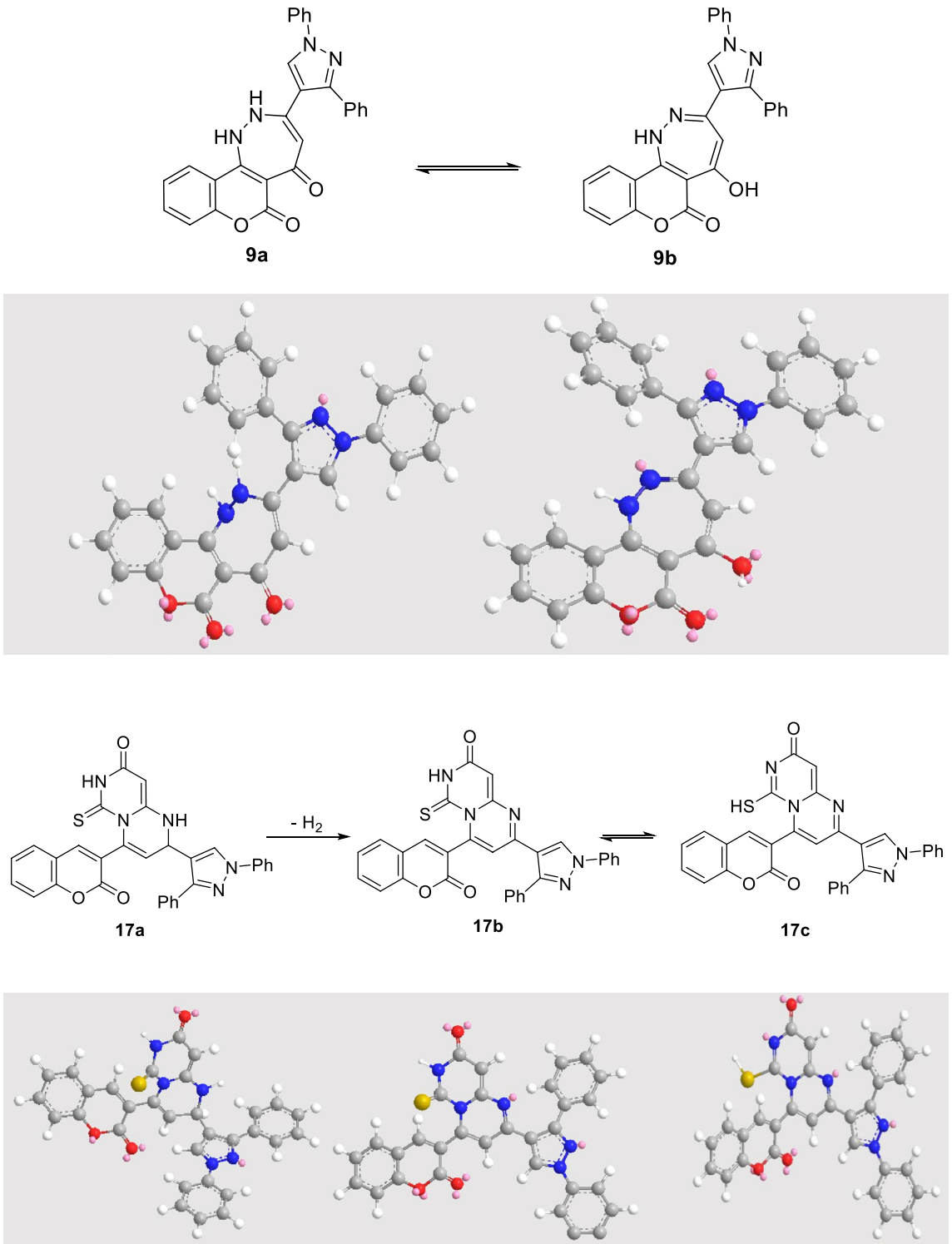

Fig. 6 Structures of compounds **9** and **17**

Table 3 Cytotoxic activity of some compounds against human tumors

Compound	In vitro cytotoxicity IC_{50} (μM) •	
	HePG-2	MCF-7
Doxorubicin	4.50 ± 0.3	4.17 ± 0.2
3	68.96 ± 3.3	81.57 ± 4.1
6	36.50 ± 2.3	70.18 ± 3.6
9	12.68 ± 1.0	9.16 ± 0.7
10	56.24 ± 3.0	51.72 ± 2.8
12	43.07 ± 2.6	26.28 ± 1.9
14	59.12 ± 3.1	38.91 ± 2.2
15	30.61 ± 2.1	45.05 ± 2.5
17	19.32 ± 1.5	14.34 ± 1.2

IC_{50} (μM): 1–10 (very strong), 11–20 (strong), 21–50 (moderate), 51–100 (weak), and above 100 (non-cytotoxic)

5-(2-(1,3-Diphenyl-1H-pyrazol-4-yl)vinyl)-2-thioxo-2,3-dihydro-4H-chromeno[4,3-d]pyrimidin-4-one (12)

A solution of Chalcone **3** (0.01 mol), thiourea (0.01 mol) and sodium ethoxide (0.01 mol Na/10 mL ethanol) in absolute ethanol (10 mL) was refluxed for 6 h. After cooling, the contents were poured onto ice-cold water and then acidified with dil. HCl (10%). The solid obtained was filtered off and pale yellow crystals were obtained after crystallization from ethanol, mp. 182–184 °C, yield 88%. IR: 3200 (NH), 1689 (C = O), 1622 (C = N), 1222 (C = S). ^{1}H NMR (300 MHz, DMSO-d_6): 12.20 (br.s, 1H, NH, exchangeable), 9.20 (s, 1H, C5-H pyrazole), 7.94–6.41 (m, 16H, Ar–H + CH = CH). MS, *m/z* (%): 474 ($M^{+\cdot}$, 12), 431 (27), 427 (52), 401 (19), 331 (100), 302 (22), 248 (50), 170 (32), 135 (24), 103 (43), 92 (39), 91 (28), 77 (94). Anal. Calcd. for $C_{28}H_{18}N_4O_2S$ (474.54): C, 70.87; H, 3.82; N, 11.81. found: C, 70.72; H, 3.74; N, 11.84%.

3-(7-(1,3-Diphenyl-1H-pyrazol-4-yl)-3-thioxo-3,4-dihydro-2H-1,2,4-triazepin-5-yl)-2H-chromen-2-one (14)

A solution of **3** (0.01 mol) and thiosemicarbazide (0.01 mol) in dioxane (15 mL) was refluxed for 8 h (TLC). The reaction mixture was poured onto ice-cold water, the separated solid was filtered off and yellow crystals were obtained after crystallization from ethanol, mp. 218–220 °C, yield 67%. IR: 3150 (NH), 1721 (C = O), 1656 (C = N), 1231 (C = S). ^{1}H NMR (300 MHz, DMSO-d_6): 11.38 (br.s, 2H, 2NH, exchangeable), 9.27 (s, 1H, C5-H pyrazole), 8.64 (s, 1H, C4-H coumarin), 8.23 (s, 1H, C6-H triazepin), 7.99–7.36 (m, 14H, Ar–H). MS, *m/z* (%): 489 ($M^{+\cdot}$, 5), 453 (7), 419 (12), 245 (51), 195 (10), 115 (22), 89 (34), 77 (100). Anal. Calcd. for $C_{28}H_{19}N_5O_2S$ (489.55): C, 68.70; H, 3.91; N, 14.31. found: C, 68.59; H, 3.85; N, 14.35%.

3-(4-(1,3-Diphenyl-1H-pyrazol-4-yl)-1H-benzo[b][1,4]diazepin-2-yl)-2H-chromen-2-one (15)

A solution of Chalcone **3** (0.01 mol) and 2-aminoaniline (0.01 mol) in dioxane (15 mL) was refluxed for 8 h (TLC). The reaction mixture was poured onto ice-cold water. The precipitated solid was filtered off and dark yellow crystals were obtained after crystallization from ethanol, mp. 212–214 °C, yield 84%. IR: 3160 (NH), 1721 (C = O coumarin), 1651 (C = N). ^{1}H NMR (300 MHz, DMSO-d_6): 12.50 (br.s, 1H, NH, exchangeable), 9.27 (s, 1H, C5-H pyrazole), 8.64 (s, 1H, C4-H coumarin), 7.99–7.00 (m, 19H, Ar–H + C3-H diazepin). MS, *m/z* (%): 506 ($M^{+\cdot}$, 8), 505 (10), 467 (9), 335 (16), 307 (23), 258 (18), 184 (33),

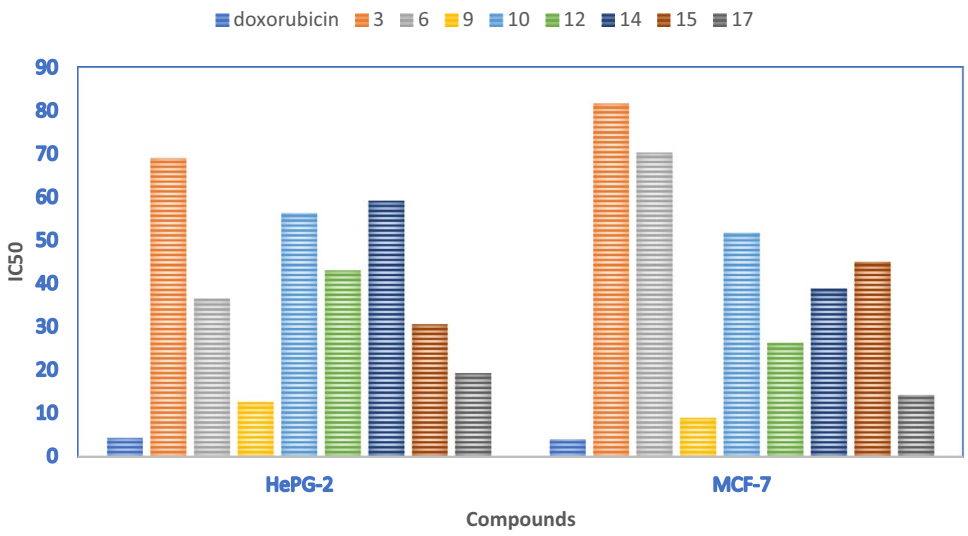

Fig. 7 IC_{50} of the tested compounds

103 (33), 91 (38), 77 (100). Anal. Calcd. for $C_{33}H_{22}N_4O_2$ (506.57): C, 78.25; H, 4.38; N, 11.06. found: C, 78.12; H, 4.30; N, 11.00%.

2-(1,3-Diphenyl-1H-pyrazol-4-yl)-4-(2-oxo-2H-chromen-3-yl)-6-thioxo-6,7-dihydro-8H-pyrimido[1,6-a]pyrimidin-8-one (17)

An equimolar mixture of **3** and 6-aminothiouracil (0.01 mol) in dioxane (15 mL) containing piperidine (0.1 mL) was refluxed for 8 h (TLC). The solid was filtered off and yellow crystals were obtained after crystallization from ethanol, mp. 218–220 °C, yield 88%. IR: 3316 (NH), 1716, 1690 (C = O), 1277 (C = S). ^{1}H NMR (300 MHz, DMSO-d_6): 12.10 (br.s, 1H, NH, exchangeable), 9.28 (s, 1H, C5-H pyrazole), 8.65 (s, 1H, C4-H coumarin), 8.08–7.25 (m, 15H, Ar–H + C-H pyrimidinone), 5.49 (s, 1H, C-H pyrimidine). MS, *m/z* (%): 541 ($M^{+\cdot}$, 45), 538 (41), 457 (33), 377 (50), 310 (82), 270 (94), 232 (100), 197 (81), 146 (99), 118 (91), 94 (37), 67 (70). Anal. Calcd. for $C_{31}H_{19}N_5O_3S$ (541.59): C, 68.75; H, 3.54; N, 12.93. found: C, 68.60; H, 3.47; N, 12.90%.

Cytotoxicity assay

Materials and methods

Hepatocellular carcinoma (HePG-2) and mammary gland breast cancer (MCF-7). The cell lines were obtained from ATCC via Holding company for biological products and vaccines (VACSERA), Cairo, Egypt. Doxorubicin was used as a standard anticancer drug for comparison. The reagents are RPMI-1640 medium, MTT, DMSO (sigma co., St. Louis, USA), and fetal bovine serum (GIBCO, UK).

MTT assay

The cell lines mentioned above were used to determine the inhibitory effects of compounds on cell growth using the MTT assay [50, 51]. This colorimetric assay is based on the conversion of the yellow tetrazolium bromide (MTT) to a purple formazan derivative by mitochondrial succinate dehydrogenase in viable cells. Cell lines were cultured in RPMI-1640 medium with 10% fetal bovine serum. Antibiotics added were 100 units/ml penicillin and 100 µg/ml streptomycin at 37 °C in a 5% CO_2 incubator. The cell lines were seed in a 96-well plate at a density of 1.0×10^4 cells/well. at 37 °C for 48 h under 5% CO_2. After incubation, the cells were treated with different concentrations of compounds and incubated for 24 h. After 24 h of drug treatment, 20 µl of MTT solution at 5 mg/ml was added and incubated for 4 h. Dimethyl sulfoxide (DMSO) in volume of 100 µl is added into each well to dissolve the purple formazan formed. The colorimetric assay is measured and recorded at absorbance of 570 nm using a plate reader (EXL 800, USA). The relative cell viability in percentage was calculated as (A_{570} of treated samples/A_{570} of untreated sample) × 100.

Supplementary Information The online version contains supplementary material available at https://doi.org/10.1007/s13738-021-02298-6.

Declarations

Conflict of interest The authors declare no conflict of interest.

References

1. B. Orlikova, D. Tasdemir, F. Golais, M. Dicato, M. Diederich, Genes Nutr. **6**, 125 (2011)
2. R. Kenchappa, Y.D. Bodke, A. Chandrashekar, M.A. Sindhe, S.K. Peethambar, Arabian J. Chem. **10**, S3895 (2017)
3. A.D. Singh, A. Kumar, S. Saini, H. Prabha, Asian Pacific. J. Health Sci. **4**, 84 (2017)
4. K.N. Anees Rahman, J. Haribabu, C. Balachandran, N.S.P. Bhuvanesh, R. Ramasamy Karvembu, A. Sreekanth, Polyhedron **135**, 26 (2017)
5. M.M. Abdou, Arab. J. Chem. **10**, S3664 (2017)
6. K.N.M. Halim, S.K. Ramadan, S.A. Rizk, M.A. El-Hashash, Synth. Commun. **50**(8), 1159 (2020)
7. S.K. Ramadan, K.N.M. Halim, S.A. Rizk, M.A. El-Hashash, J. Iran. Chem. Soc. **17**, 1575 (2020)
8. K.N.M. Halim, S.A. Rizk, M.A. El-Hashash, S.K. Ramadan, J. Heterocycl. Chem. **58**(2), 636 (2021)
9. S.K. Ramadan, W.S.I. Abou-Elmagd, Synth. Commun. **48**(18), 2409 (2018)
10. S.K. Ramadan, A.K. El-Ziaty, R.S. Ali, J. Heterocycl. Chem. **58**, 290 (2021)
11. S.K. Ramadan, S.S. Shaban, A.I. Hashem, Synth. Commun. **50**(2), 185 (2020)
12. E.A.E. El-Helw, A.A. El-Badawy, J. Heterocycl. Chem. **57**(6), 2354 (2020)
13. S.K. Ramadan, E.A.E. El-Helw, H.A. Sallam, Heterocycl. Commun. **25**(1), 107 (2019)
14. S.K. Ramadan, H.A. Sallam, J. Heterocycl. Chem. **55**(8), 1942 (2018)
15. W.S.I. Abou-Elmagd, A.K. El-Ziaty, M.I. Elzahar, S.K. Ramadan, A.I. Hashem, Synth. Commun. **46**, 1197 (2016)
16. E.A.E. El-Helw, M.M. Gado, A.K. El-Ziaty, J. Iran. Chem. Soc. **17**, 1479 (2020)
17. S. Maddila, S. Gorle, N. Seshadri, P. Lavanya, S.B. Jonnalagadda, Arab. J. Chem. **9**, 681 (2016)
18. D. Kumar, S.I. Khan, B.L. Tekwani, P. Ponnan, D.S. Rawat, Eur. J. Med. Chem. **89**, 490 (2015)
19. C.M. Bhalgat, M.I. Ali, B. Ramesh, G. Ramu, Arab. J. Chem. **7**, 986 (2014)
20. P.J. Chen, A. Yang, Y.F. Gu, X.S. Zhang, K.P. Shao, D.Q. Xue, P. He, T.F. Jiang, Q.R. Zhang, H.M. Liu, Bioorg. Med. Chem. Lett. **24**, 2741 (2014)
21. S.I. Pretorius, W.J. Breytenbach, C. De. Kock, P.J. Smith, D.D. N'Da, Bioorg. Med. Chem. **21**, 269 (2013)
22. D.G. Powers, D.S. Casebier, D. Fokas, W.J. Ryan, J.R. Troth, D.L. Coffen, Tetrahedron **54**, 4085 (1998)

23. S.A. Rizk, M.A. El-Hashash, K.K. Mostafa, Egypt. J. Chem. **51**, 116 (2008)
24. S.A. Rizk, G. Elsayed, M.A. El-Hashash, J. Iran. Chem. Soc. **15**, 2093 (2018)
25. M.A. El-Hashash, S.A. Rizk, F.A. El-Bassiouny, D.B. Guirguis, S.M. Khairy, L. Guirguis, Egypt J. Chem. **60**, 407 (2017)
26. M.A. El-Hashash, K.M. Darwish, S.A. Rizk, F.A. El-Basiouny, Pharmaceuticals **4**(7), 1032 (2011)
27. A.M. Youssef, A.K. El-Ziaty, W.S.I. Abou-Elmagd, S.K. Ramadan, J. Heterocycl. Chem. **52**(1), 278 (2015)
28. A.R.I. Morsy, S.K. Ramadan, M.M. Elsafty, Med. Chem. Res. **29**, 979 (2020)
29. S.K. Ramadan, E.Z. Elrazaz, K.A.M. Abouzid, A.M. El-Naggar, RSC Adv. **10**, 29475 (2020)
30. A.M. El-Naggar, S.K. Ramadan, Synth. Commun. **50**(14), 2188 (2020)
31. S.K. Ramadan, A.I. Hashem, W.S.I. Abou-Elmagd, A.K. El-Ziaty, J. Heterocycl. Chem. **54**(6), 3711 (2017)
32. S.K. Ramadan, E.A.E. El-Helw, J. Chem. Res. **42**, 332 (2018)
33. N.M. Gad, W.S.I. Abou-Elmagd, D.S.A. Haneen, S.K. Ramadan, Synth. Commun. **51**(9), 1384 (2021)
34. S.K. Ramadan, A.K. El-Ziaty, E.A.E. El-Helw, Synth. Commun. **51**(8), 1272 (2021)
35. E.A.E. El-Helw, A.I. Hashem, Synth. Commun. **50**(7), 1046 (2020)
36. E.A.E. El-Helw, A.R.I. Morsy, A.I. Hashem, J. Heterocycl. Chem. **58**(4), 1003 (2021)
37. A.A. El-Badawy, A.S. Elgubbi, E.A.E. El-Helw, J. Sulfur Chem. **42**, 295 (2021)
38. H.A. Sallam, A.S. Elgubbi, E.A.E. El-Helw, Synth. Commun. **50**(13), 2066 (2020)
39. M.S. Salem, E.A.E. El-Helw, H.A.Y. Derbala, Russ. J. Bioorg. Chem. **46**(1), 77 (2020)
40. E.A.E. El-Helw, H.A. Sallam, A.S. Elgubbi, Synth. Commun. **49**(20), 2651 (2019)
41. S.K. Ramadan, E.A.E. El-Helw, M.E. Azab, Russ. J. Org. Chem. **55**(12), 1940 (2019)
42. P. Rathelot, N. Azas, H. El-Kashef, F. Delmas, C.D. Giorgio, P. Timon-David, J. Maldonado, P. Vanelle, Eur. J. Med. Chem. **37**, 671 (2002)
43. J.-P. Li, J.-K. Qiu, H.-J. Li, G.-S. Zhang, J. Chin. Chem. Soc. **58**, 268 (2011)
44. F. El-Taib Heakal, S.A. Rizk, A.E. Elkholy, J. Mol. Struct. **1152**, 328 (2018)
45. L.E. Chirlian, M.M. Francl, J. Comput. Chem. **8**, 894 (1987)
46. A.E. Elkholy, S.A. Rizk, A.M. Rashad, J. Mol. Struct. **1175**, 788 (2019)
47. R. Dhingra, V. Margulets, S.R. Chowdhury, J. Thliveris, D. Jassal, P. Fernyhough, G.W. Dorn, L.A. Kirshenbaum, Proc. Natl. Acad. Sci. USA **111**, E5537 (2014)
48. B. Kalyanaraman, Redox Biol. **29**, 101394 (2020)
49. X. Fang, H. Wang, D. Han, E. Xie, X. Yang, J. Wei, S. Gu, F. Gao, N. Zhu, X. Yin, Q. Cheng, P. Zhang, W. Dai, Proc. Natl. Acad. Sci. U. S. A. **116**, 2672 (2019)
50. T. Mosmann, J. Immunol. Methods **65**, 55 (1983)
51. F. Denizot, R. Lang, J. Immunol. Methods **22**, 271 (1986)